High pressure effects on the crystal and magnetic structure of $La_{0.7}Sr_{0.3}MnO_3$

2004 J. Phys.: Condens. Matter 16 6755

(http://iopscience.iop.org/0953-8984/16/37/011)

INSTITUTE OF PHYSICS PUBLISHING JOURNAL OF PHYSICS: CONDENSED MATTER

J. Phys.: Condens. Matter **16** (2004) 6755–6762 PII: S0953-8984(04)84790-8

High pressure effects on the crystal and magnetic structure of $La_{0.7}Sr_{0.3}MnO_3$

D P Kozlenko[1,2], I N Goncharenko[3], B N Savenko[2] and V I Voronin[4]

[1] ISIS Facility, Rutherford Appleton Laboratory, Chilton, Didcot, Oxon OX11 0QX, UK
[2] Frank Laboratory of Neutron Physics, Joint Institute for Nuclear Research, 141980 Dubna Moscow Region, Russia
[3] Laboratoire Léon Brillouin, CEA-CNRS, CE Saclay, 91191 Gif-sur-Yvette Cedex, France
[4] Institute for Metal Physics, Ural Division of RAS, 620219 Ekaterinburg, Russia

Received 9 August 2004
Published 3 September 2004
Online at stacks.iop.org/JPhysCM/16/6755
doi:10.1088/0953-8984/16/37/011

Abstract

The crystal and magnetic structure of manganite $La_{0.7}Sr_{0.3}MnO_3$ has been studied in the pressure range 0–7.5 GPa and the temperature range 4–300 K. The ferromagnetic state of $La_{0.7}Sr_{0.3}MnO_3$ remains stable in the whole studied pressure range. The Curie temperature increases as $dT_C/dP = 4.3$ K GPa^{-1}. Unlike the manganites with orthorhombic crystal structure, the pressure-induced increase of T_C in $La_{0.7}Sr_{0.3}MnO_3$ having the rhombohedral crystal structure of $R\bar{3}c$ symmetry may be explained by modification of structural parameters only. The difference between the properties of manganites with rhombohedral and orthorhombic structures under high pressure is discussed in terms of the symmetry of MnO_6 octahedra.

1. Introduction

Manganites of perovskite type $A_{1-x}A'_xMnO_3$ (A—rare earth, A′—alkali earth elements) exhibit rich magnetic and electronic phase diagrams depending on the A-site elements and their ratio. They have attracted considerable interest with respect to the recently discovered colossal magnetoresistance (CMR) effect [1]. For the optimum doping range $x \sim 0.3$ manganites generally exhibit a ferromagnetic metallic state below the Curie temperature T_C which is governed by the double-exchange interaction [2–4]. The ferromagnetic arrangement of the localized t_{2g} spins is mediated by the itinerant e_g electrons via the on-site Hund's rule coupling J_H. The magnetic and transport properties of double-exchange ferromagnets are controlled by the one-electron bandwidth W, which is proportional to the Mn–O–Mn electron transfer integral and $T_C \propto W$ in the strong coupling limit ($J_H \gg W$) [5]. The bandwidth can be effectively tuned by the 'internal' pressure (variation of the average A-site ionic radius $\langle r_A \rangle$) or high external pressure via changes of the Mn–O distance and the Mn–O–Mn bond angle. Both the increase of $\langle r_A \rangle$ and the application of external pressure lead to the increase of T_C [6–9].

The one-electron bandwidth also depends substantially on the electron–phonon coupling effects coming from the long range cooperative Jahn–Teller (JT) distortion of MnO_6 octahedra [10]. Such effects are pronounced in the optimally doped manganites with the orthorhombic crystal structure of the *Pnma* symmetry ($\langle r_A \rangle < 1.22$ Å) and strongly reduced for those with the rhombohedral structure of the $R\bar{3}c$ symmetry ($\langle r_A \rangle > 1.22$ Å), as found in the study of compounds $La_{2/3}(Ca_{1-x}Sr_x)_{1/3}MnO_3$ [11].

The investigations of manganites $A_{0.67}A'_{0.33}MnO_3$ (A = La, Pr, Sm, Nd, Y; A′ = Ca, Sr) having the orthorhombic crystal structure of the *Pnma* symmetry with 1.124 Å $< \langle r_A \rangle <$ 1.147 Å [9] and $La_{0.75}Ca_{0.25}MnO_3$ ($\langle r_A \rangle = 1.207$ Å) [12] revealed that the observed variation of T_C (which coincides with the insulator–metal transition temperature T_{IM}) under high pressure does not correspond to that expected from the modification of structural parameters only. The experimental dT_C/dP value in the low pressure range was about an order of magnitude larger than the estimation obtained from the consideration of structural parameter variation. The rest of the observed bandwidth modification was attributed to the electron–phonon coupling effects. The application of high pressure also leads to the suppression of the initial FM state and appearance of the A-type layered antiferromagnetic (AFM) state in manganites $La_{0.67}Ca_{0.33}MnO_3$ [13] and $Pr_{0.7}Ca_{0.3}Mn_{0.9}Fe_{0.1}O_3$ [14] with the orthorhombic crystal structure of *Pnma* symmetry.

The high pressure effects on the structural and magnetic properties of the optimally doped manganites with the rhombohedral crystal structure of the $R\bar{3}c$ symmetry are less studied. In this case the static long range cooperative Jahn–Teller distortion is forbidden by the symmetry and the relevant electron–phonon coupling effects which would affect the one-electron bandwidth are negligible. Hence, the interplay between the variation of the structural parameters and the relevant modification of the one-electron bandwidth and T_C in the optimally doped manganites ($x \sim 0.3$) under high pressure may be explored directly by the study of high pressure effects on the crystal and magnetic structure of rhombohedral manganites.

Manganites $La_{1-x}Sr_xMnO_3$ have the rhombohedral structure of the $R\bar{3}c$ symmetry for $x > 0.18$ [15]. The compound $La_{0.7}Sr_{0.3}MnO_3$ exhibits the metallic-like temperature behaviour of resistivity and transforms to the ferromagnetic (FM) state at $T_C \sim 370$ K [15]. Magnetic and transport properties of $La_{0.7}Sr_{0.3}MnO_3$ were studied in the moderate pressure range up to 1 GPa only [16]. It was found that the T_C increases under high pressure with $dT_C/dP \approx 5$ K GPa^{-1}. This value is much smaller in comparison with that obtained in the same pressure range for the manganites with a close chemical content but the orthorhombic crystal structure—$La_{0.75}Ca_{0.25}MnO_3$, $dT_C/dP \approx 23$ K GPa^{-1} [12] and $La_{0.67}Ca_{0.33}MnO_3$, $dT_C/dP \approx 13$ K GPa^{-1} [9, 17], respectively.

In the present work, the interplay between the structural and magnetic properties of manganite $La_{0.7}Sr_{0.3}MnO_3$ is investigated by neutron diffraction in the extended pressure range up to 7.5 GPa.

2. Experimental details

The compound $La_{0.7}Sr_{0.3}MnO_3$ was prepared by a solid state reaction as described in detail in [18].

The crystal structure of $La_{0.7}Sr_{0.3}MnO_3$ was investigated using the Pearl/HiPr diffractometer at the ISIS pulsed neutron spallation source (Rutherford Appleton Laboratory, UK). The Paris–Edinburgh high pressure cell [19] was used with a 4:1 volume mixture of fully deuterated methanol–ethanol as a pressure transmitting medium. A TiZr encapsulated gasket of 90 mm^3 initial volume was used to attain nearly hydrostatic compression of the sample in the studied pressure range [20]. For the pressure determination, NaCl as a reference material [21]

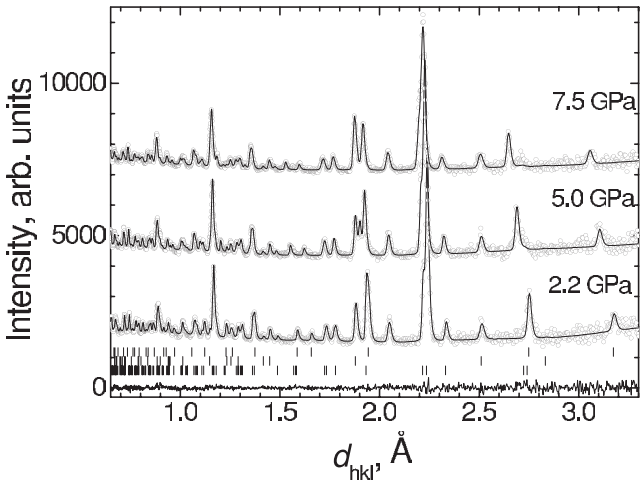

Figure 1. Neutron diffraction patterns of $La_{0.7}Sr_{0.3}MnO_3$, measured at the Pearl/HiPr diffractometer at $P = 2.2$, 5.0 and 7.5 GPa and ambient temperature and processed by the Rietveld method. Experimental points, calculated profiles and difference curve (for $P = 2.2$ GPa, bottom) are shown. The ticks below represent calculated positions of diffraction peaks of $La_{0.7}Sr_{0.3}MnO_3$ (bottom row), tungsten carbide (WC) coming from the anvils of the high pressure cell (middle row) and NaCl used as reference material for pressure determination (top row) at $P = 2.2$ GPa.

was admixed to the sample in ∼1:2 volume proportion. Diffraction patterns were collected by a detector bank covering the scattering angle range $83° < 2\theta < 97°$. The experiments were performed in the pressure range 0–7.5 GPa at ambient temperature. Typical data collection time was about 3 h. The diffraction data were analysed by the Rietveld method using the general structure analysis system (GSAS) [22].

The magnetic structure of $La_{0.7}Sr_{0.3}MnO_3$ was investigated with the G6.1 diffractometer at the Orphée reactor (Laboratoire Léon Brillouin, France). The incident neutron wavelength was 4.74 Å. The sample with a volume of about 1 mm^3 was loaded in the sapphire anvil high pressure cell [23]. Several tiny ruby chips were placed at different points on the sample surface and the pressure was determined by a standard ruby fluorescence technique. Measurements of the pressure distribution on the sample yield typical pressure inhomogeneities of ±5%. Neutron focusing systems [24] and special cadmium protection were used to increase the neutron flux at the sample position and achieve a low background level, respectively. The measurements were performed in the pressure range 0–5.8 GPa and temperature range 4–295 K. A typical data collection time was about 4 h. The diffraction data were analysed by the Rietveld method using the FULLPROF programme [25].

3. Results

Neutron diffraction patterns of $La_{0.7}Sr_{0.3}MnO_3$ measured at different pressures and ambient temperature at the Pearl/HiPr diffractometer are shown in figure 1. Over the whole studied pressure range (0–7.5 GPa) $La_{0.7}Sr_{0.3}MnO_3$ retains the rhombohedral structure of $R\bar{3}c$ symmetry. The structural parameters obtained from the Rietveld refinement of the diffraction data at selected pressures and ambient temperature are presented in table 1. The hexagonal axis setting was used for the refinement. The values of structural parameters at ambient pressure and temperature agree well with ones obtained in [26].

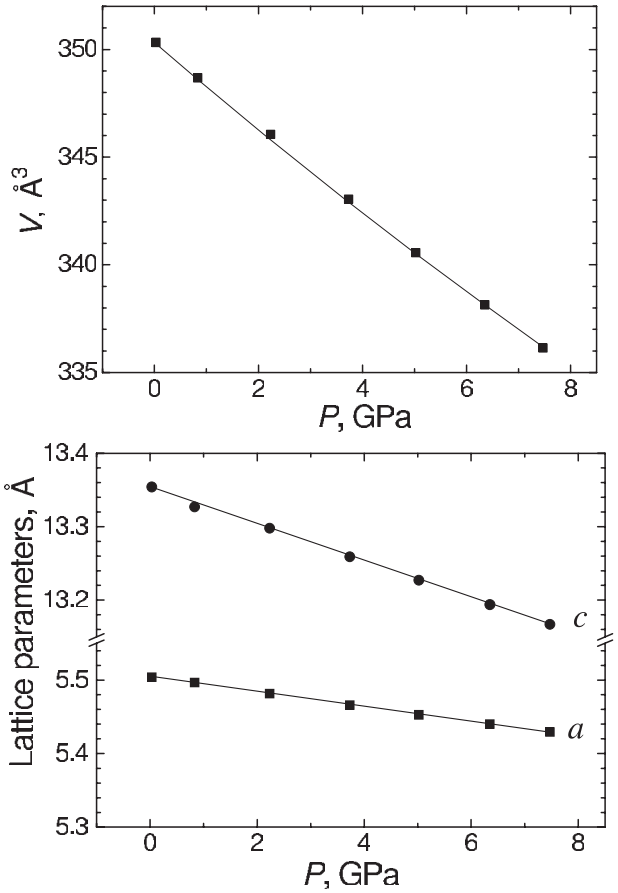

Figure 2. Pressure dependence of the unit cell volume of $La_{0.7}Sr_{0.3}MnO_3$ fitted by the third-order Birch–Murnaghan equation of state (1) and lattice parameters fitted by linear functions (solid lines). The error bars are within the symbol sizes.

Table 1. Structural parameters of $La_{0.7}Sr_{0.3}MnO_3$ at selected pressures and ambient temperature. The hexagonal axis setting was used. The atomic positions are Mn—6(b) (0, 0, 0), La/Sr—6(a) (0, 0, 0.25) and O—18(e) (x, 0, 0.25) of the space group $R\bar{3}c$. Values of Mn–O bond lengths and Mn–O–Mn bond angles are also presented.

P (GPa)	0	2.2	5.0	7.5
a (Å)	5.5038(4)	5.4816(2)	5.4527(2)	5.4294(3)
c (Å)	13.354(2)	13.298(1)	13.227(1)	13.167(1)
O, x	0.4569(6)	0.4585(4)	0.4593(4)	0.4612(4)
Mn–O (Å)	1.954(2)	1.945(1)	1.934(1)	1.925(1)
Mn–O–Mn	166.1(2)°	166.6(1)°	166.8(1)°	167.4(1)
R_p (%)	11.76	6.76	6.06	5.89
R_{wp} (%)	6.47	3.99	3.68	3.82

The obtained unit cell volume versus pressure dependence for $La_{0.7}Sr_{0.3}MnO_3$ is shown in figure 2. The compressibility data were fitted by the third-order Birch–Murnaghan equation of state [27]:

$$P = \tfrac{3}{2}B_0(x^{-7/3} - x^{-5/3})[1 + \tfrac{3}{4}(B' - 4)(x^{-2/3} - 1)], \quad (1)$$

where $x = V/V_0$ is the relative volume change, V_0 is the unit cell volume at $P = 0$, and B_0 and B' are the bulk modulus ($B_0 = -V(\mathrm{d}P/\mathrm{d}V)_T$) and its pressure derivative ($B' = (\mathrm{d}B_0/\mathrm{d}P)_T$). The calculated values $B_0 = 167(5)$ GPa and $B' = 4(1)$ are comparable with those

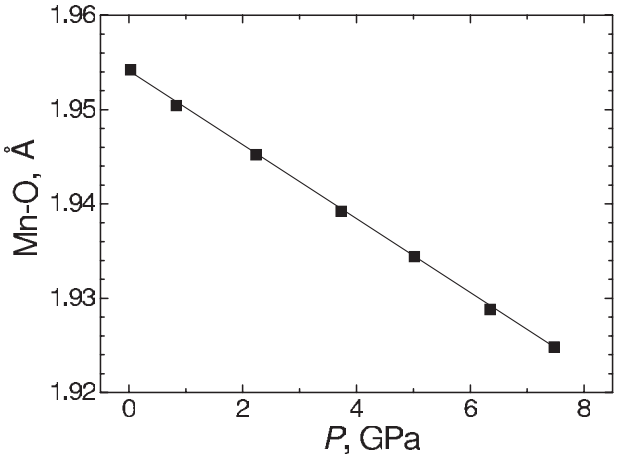

Figure 3. Mn–O bond length of $La_{0.7}Sr_{0.3}MnO_3$ as a function of pressure. The solid line represents a linear fit to the experimental data. The error bars are within the symbol sizes.

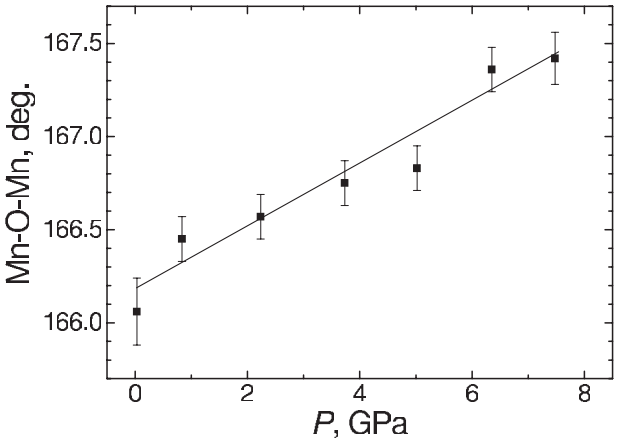

Figure 4. Mn–O–Mn bond angle of $La_{0.7}Sr_{0.3}MnO_3$ as a function of pressure. The solid line represents a linear fit to the experimental data.

$B_0 = 178$ GPa and $B' = 4$ determined for the manganite $La_{0.75}Ca_{0.25}MnO_3$ [28] with the orthorhombic structure of *Pnma* symmetry. The pressure dependence of lattice parameters is also shown in figure 2. The linear compressibilities $k_i = -(1/a_{i0})(\mathrm{d}a_i/\mathrm{d}P)_T$ $(a_i = a, c)$ along the a and c axes are nearly the same, $k_a \approx k_c = 0.0018(2)$ GPa^{-1}. These values are close to those reported for lattice parameters of $La_{0.75}Ca_{0.25}MnO_3$ [28].

In the rhombohedral structure of $La_{0.7}Sr_{0.3}MnO_3$ the MnO_6 octahedra consist of Mn–O bonds of equal length and Mn–O–Mn bond angles of equal value. With the pressure increase the Mn–O bond length decreases (figure 3) and the Mn–O–Mn bond angle increases (figure 4) nearly linearly.

Neutron diffraction patterns of $La_{0.7}Sr_{0.3}MnO_3$ obtained at $P = 4.5$ GPa and temperatures 300 and 4 K at the G6.1 diffractometer are shown in figure 5. An increase of the intensity of the diffraction peaks (012) and (110)/(104) with the temperature decrease from 300 to 4 K due to the FM contribution was observed in the whole studied pressure range up to 5.8 GPa. The temperature dependences of the Mn magnetic moment at different pressures determined from the Rietveld refinement of the diffraction data are shown in figure 6. The obtained values of Mn magnetic moments at high pressures, $\mu \approx 2.4(1)\ \mu_B$ at $T = 300$ K and $\mu \approx 3.4(1)\ \mu_B$ at $T = 4$ K, are close to those obtained at ambient pressure [15, 20]. In order to obtain the pressure dependence of the Curie temperature, $\mu(T)$ data were fitted by the function

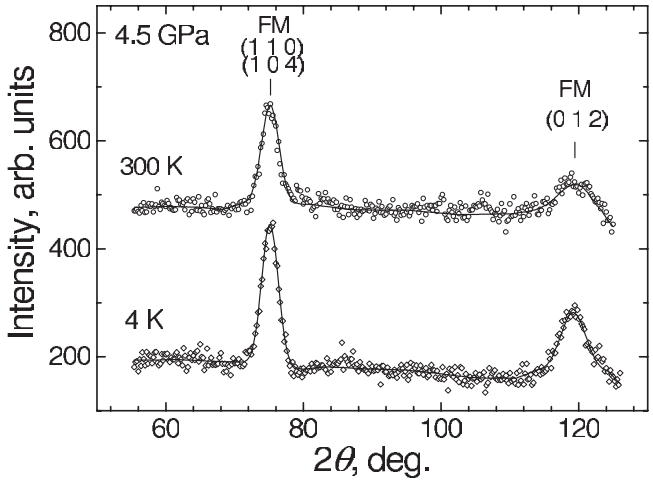

Figure 5. Neutron diffraction patterns of $La_{0.7}Sr_{0.3}MnO_3$, measured at the G6.1 diffractometer at $P = 4.5$ GPa and $T = 300$ and 4 K and processed by the Rietveld method. Experimental points and calculated profiles are shown. Indices of observed diffraction peaks are given.

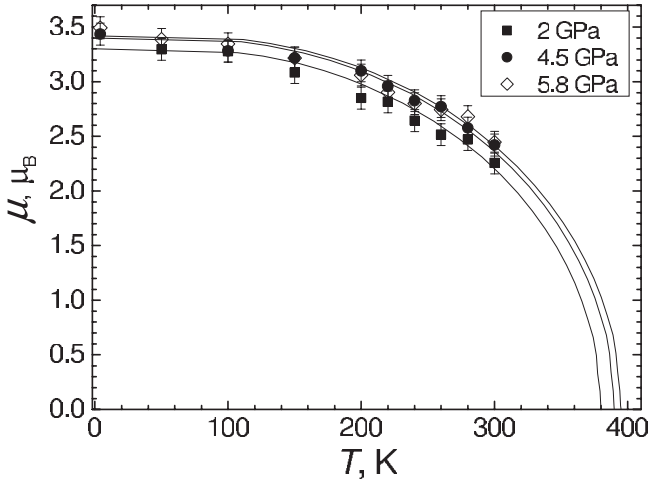

Figure 6. Temperature dependences of the Mn magnetic moment at different pressures fitted by the function described by equation (2).

describing the temperature dependence of the magnetic moment of ferromagnetic materials in the molecular field model [29]:

$$\frac{\mu}{\mu_0} = B_S\left(\frac{3S}{S+1}\frac{\mu}{\mu_0}\frac{T_C}{T}\right), \tag{2}$$

where B_S is the Brillouin function, S is the spin of the system ($S = 3/2$) and μ_0 is the magnetic moment at $T = 0$. The obtained pressure dependence of T_C is shown in figure 7. It increases nearly linearly from $T_C = 370$ K at $P = 0$ (this point was taken from the study of magnetic properties of this sample at ambient pressure [18]) to 395 K at $P = 5.8$ GPa with $dT_C/dP = 4.3 \pm 1.1$ K GPa^{-1}. This value agrees well within the experimental error with $dT_C/dP = 5.3$ K GPa^{-1} obtained in the study of $La_{0.7}Sr_{0.3}MnO_3$ in the pressure range up to 1 GPa [16].

4. Discussion

The dependence of the one-electron bandwidth $W \sim T_C$ on the Mn–O bond length l can be expressed as $W \sim l^{-3.5}$ and its dependence on the Mn–O–Mn bond angle φ can be written, to

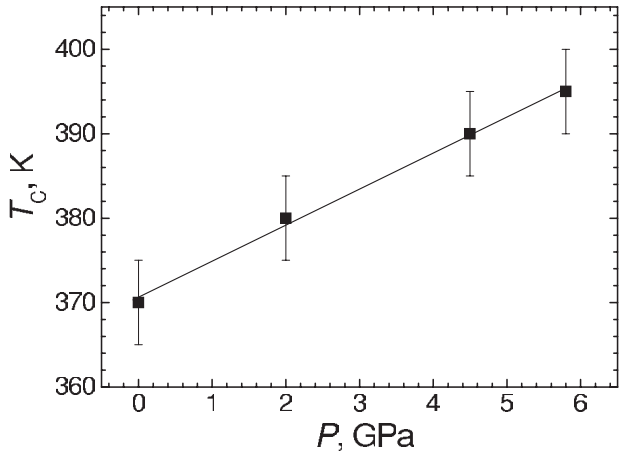

Figure 7. Curie temperature of $La_{0.7}Sr_{0.3}MnO_3$ as a function of pressure. The solid line represents a linear fit to the experimental data.

first order, as $W \sim \cos^2(\varphi)$ [9, 30]. Therefore, one obtains [9]

$$(1/T_C)(dT_C/dP) = 3.5k_l - 2\tan(\varphi)\varphi k_\varphi, \tag{3}$$

where $k_l = -(1/l_0)(dl/dP)$ and $k_\varphi = (1/\varphi_0)(d\varphi/dP)$. Equation (3) gives $(1/T_C)(dT_C/dP) = 0.0084$ GPa^{-1} and $dT_C/dP = 3.1$ K GPa^{-1} using the values of $k_l = 0.0020$ GPa^{-1} and $k_\varphi = 0.0010$ GPa^{-1}, obtained from the present structural data.

The calculated value of $dT_C/dP = 3.1$ K GPa^{-1} is in agreement with the experimental one 4.3 K GPa^{-1}. Thus, the pressure behaviour of T_C in $La_{0.7}Sr_{0.3}MnO_3$ can be explained in terms of the modification of structural parameters only.

One of the important factors responsible for the difference between the properties of the manganites with a rhombohedral and orthorhombic crystal structure and the optimal doping level $x \sim 0.3$ is the relevant symmetry of MnO_6 octahedra. In the crystal structure of manganites with the rhombohedral $R\bar{3}c$ symmetry MnO_6 octahedra are isotropic with equal Mn–O bond lengths and Mn–O–Mn angles and the electron–phonon coupling effects are negligible due to the absence of the static long-range cooperative JT distortion. In the crystal structure of the compounds with a lower orthorhombic *Pnma* symmetry there are three pairs of Mn–O bonds of different length and two different Mn–O–Mn bond angles. The enhanced electron–phonon coupling arising from the static cooperative JT distortion modifies the one-electron bandwidth and its high pressure behaviour becomes more complicated and cannot be described by the structural effects only, as was found for manganites $A_{0.67}A'_{0.33}MnO_3$ (A = La, Pr, Sm, Nd; Y, A′ = Ca, Sr) with 1.124 Å $< \langle r_A \rangle <$ 1.147 Å [9] and $La_{0.75}Ca_{0.25}MnO_3$ ($\langle r_A \rangle =$ 1.207 Å) [12]. The study of manganites $La_{2/3}(Ca_{1-y}Sr_y)_{1/3}MnO_3$ at ambient pressure [11] also revealed that enhanced lattice effects are responsible for different properties of the samples with the orthorhombic structure in comparison with those having the rhombohedral structure.

The isotropy of the MnO_6 octahedra in the rhombohedral structure of $La_{0.7}Sr_{0.3}MnO_3$ would also be responsible for the stability of the FM state under high pressure. In the compounds $La_{0.67}Ca_{0.33}MnO_3$ [13] and $Pr_{0.7}Ca_{0.3}Mn_{0.9}Fe_{0.1}O_3$ [14] with a close chemical composition but the orthorhombic structure of *Pnma* symmetry a suppression of the FM state and the concurrent appearance of the layered A-type antiferromagnetic (AFM) state was observed at high pressure. The pressure-induced stabilization of the A-type AFM state in $La_{0.67}Ca_{0.33}MnO_3$ and $Pr_{0.7}Ca_{0.3}Mn_{0.9}Fe_{0.1}O_3$ was related to the anisotropic contraction of the MnO_6 octahedra along the crystallographic *b*-axis which creates favourable conditions for appearance of the $d_{(x^2-y^2)}$ orbital polarization, prerequisite for the A-type AFM order [13, 14].

5. Conclusions

In summary, results of our study show that the ferromagnetic state of $La_{0.7}Sr_{0.3}MnO_3$ remains stable in the investigated high pressure range and the pressure-induced increase of the Curie temperature may be explained in the framework of the double-exchange model by consideration of the structural effects only. The important factor responsible for such a behaviour is the isotropy of the MnO_6 octahedra in the rhombohedral crystal structure of $La_{0.7}Sr_{0.3}MnO_3$ which results in the absence of the static long-range cooperative JT distortion and the related electron–phonon coupling effects which strongly affect the properties of manganites with a less symmetric orthorhombic structure.

Acknowledgments

The authors thank W G Marshall and D J Francis for their help with ISIS experiments. The allocation of beamtime and financial support of the ISIS and LLB facilities and the Russian Foundation for Basic Research, grant 03-02-16879, are gratefully acknowledged.

References

[1] Dagotto E, Hotta T and Moreo A 2001 *Phys. Rep.* **344** 1
[2] Zener C 1951 *Phys. Rev.* **82** 403
[3] Anderson P W and Hasegawa H 1955 *Phys. Rev.* **100** 675
[4] De Gennes P-G 1960 *Phys. Rev.* **118** 141
[5] Furukawa N 1999 *Physics of Manganites* ed T A Kaplan and S D Mahanti (New York: Kluwer–Academic/Plenum) pp 1–38
Furukawa N 1998 *Preprint* cond-mat/9812066
[6] Hwang H Y, Cheong S-W, Radaelli P G, Marezio M and Batlogg B 1995 *Phys. Rev. Lett.* **75** 914
[7] Hwang H Y, Palstra T T M, Cheong S-W and Batlogg B 1995 *Phys. Rev.* B **52** 15046
[8] García-Muñoz J L, Fontcuberta J, Suaaidi M and Obradors X 1996 *J. Phys.: Condens. Matter* **8** L787
[9] Laukhin V, Fontcuberta J, García-Muñoz J L and Obradors X 1997 *Phys. Rev.* B **56** R10009
[10] Millis A J, Littlewood P B and Shraiman B I 1995 *Phys. Rev. Lett.* **74** 5144
[11] Mira J, Rivas J, Hueso L E, Rivadulla F, López Quintela M A, Señarís Rodríguez M A and Ramos C A 2001 *Phys. Rev.* B **65** 024418
[12] Postorino P, Congeduti A, Dore P, Sacchetti A, Gorelli F, Ulivi L, Kumar A and Sarma D D 2003 *Phys. Rev. Lett.* **91** 175501
[13] Kozlenko D P, Glazkov V P, Sadykov R A, Savenko B N, Voronin V I and Medvedeva I V 2003 *J. Magn. Magn. Mater.* **258/259** 290
[14] Kozlenko D P, Voronin V I, Glazkov V P, Medvedeva I V and Savenko B N 2004 *Phys. Solid State* **46** 484
[15] Urushibara A, Moritomo Y, Arima T, Asamitsu A, Kido G and Tokura Y 1995 *Phys. Rev.* B **51** 14103
[16] Moritomo Y, Asamitsu A and Tokura Y 1995 *Phys. Rev.* B **51** 16491
[17] Neumeier J J, Hundley M F, Thompson J D and Heffner R H 1995 *Phys. Rev.* B **52** R7006
[18] Petrov A N, Voronin V I, Norby T and Kofstad P 1999 *J. Solid State Chem.* **143** 52
[19] Besson J M, Nelmes R J, Hamel G, Loveday J S, Weill G and Hull S 1992 *Physica* B **180/181** 907
[20] Marshall W G and Francis D J 2002 *J. Appl. Crystallogr.* **135** 122
[21] Decker D L 1971 *J. Appl. Phys.* **42** 3239
[22] Von Dreele R B and Larson A C 1986 *Los Alamos National Laboratory Report No* LAUR 86 748
[23] Goncharenko I N, Glazkov V P, Irodova A V, Lavrova O A and Somenkov V A 1992 *J. Alloys Compounds* **179** 253
Goncharenko I N 2004 *High Pressure Res.* **24** 193
[24] Goncharenko I N, Mirebeau I, Molina P and Boni P 1997 *Physica* B **234–236** 1047
[25] Rodriguez-Carvajal J 1993 *Physica* B **192** 55
[26] Radaelli P G, Iannone G, Marezio M, Hwang H Y, Cheong S-W, Jorgensen J D and Argyriou D N 1997 *Phys. Rev.* B **56** 8265
[27] Birch F J 1986 *J. Geophys. Res.* **91** 4949
[28] Meneghini C, Levy D, Mobilio S, Ortolani M, Nuñez-Reguero M, Kumar A and Sarma D D 2001 *Phys. Rev.* B **65** 012111
[29] Beznosov A B, Desnenko V A, Fertman E L, Ritter C and Khalyavin D D 2003 *Phys. Rev.* B **68** 054109
[30] Harrison W A 1980 *The Electronic Structure and Properties of Solids* (San Francisco, CA: Freeman)